ISSN 1330-3651 (Print), ISSN 1848-6339 (Online) https://doi.org/10.17559/TV-20210520095227
Original scientific paper

Optimal Gear-Shifting of a Wet-Type Two-Speed Dual-Brake Transmission for an Electric Vehicle

Xinxin ZHAO*, Jinggang ZHANG, Nasser Lashgarian AZAD, Senqi TAN, Yuhan SONG

Abstract: In improving the efficiency of powertrain systems and ride comfort for electric vehicles (EVs), the transmission model is required to enable more accessible and more straightforward control of such vehicles. In this study, a wet-type, two-speed, dual-brake transmission system, as well as a new electromechanical clutch actuator, is presented for EVs. A new coordinated optimal shifting control strategy is then introduced to avoid sharp jerks during shifting processes in the transmission system. Based on a state-space model of the electromechanical clutch actuator and dual-brake transmission, we develop a linear quadratic regulator strategy by considering ride comfort and sliding friction work to obtain optimal control trajectories of the traction and shifting motors under model-based control. Simulations and bench tests are carried out to verify the performance of the proposed control laws. Results of the proposed coordinated control strategy show that noticeable improvements in terms of vehicle jerk and friction energy loss are achieved compared with an optimal control scheme only for the shifting motor as the input.

Keywords: dual-brake; linear quadratic regulator; shifting control; two-speed transmission

1 INTRODUCTION

With significant problems of environmental pollution and energy crisis, the development of electric vehicles (EVs) has been highly promoted in recent years. As a result, it is of great significance to carry out research on different types of such vehicles [1-3].The application of multi-speed transmissions for EVs can extend their range by switching speed-change gears. In addition, the overall powertrain efficiency can be improved by choosing separate gears during different driving conditions, which can keep most of the working points of the motor in high-efficiency regions. A two-speed transmission is added to the electric drivetrain for bench tests to reduce the size of the traction motor, overall powertrain mass, and manufacturing cost [4-5]. Loveday et al. [6] and Spanoudakis et al. [7] have verified the economic performance improvements offered by multi-speed transmissions for pure EVs (PEVs) and fuel-cell EVs (FCEVs), respectively. In these studies, a powertrain design involving two-speed transmission for battery EVs was presented, and all kinds of transmission systems used in traditional combustion vehicles, such as continuously variable, parallel shaft structure, and planetary gear structure transmissions, were proposed for use within battery EVs. Generally, clutch actuators can be divided into three types based on the actuating medium: hydraulic, electrohydraulic, and electromechanical. Instead of a hydraulic actuator, a novel electromechanical actuator is preferred for EV transmissions since it is more accurate, efficient, adaptable, and reliable. Liu et al. presented a new design of an electromechanical actuator with a wedge mechanism to reduce the shifting motor size and demanded power [8]. Oh et al. [9] designed a dry clutch actuator for dual-clutch transmissions (DCTs) based on the self-energizing principle. The application of two-speed transmission systems to EVs will inevitably bring the problem of shifting jerk; thus, proper strategies to control the vehicle traction motors and clutch actuators are needed to reduce the jerk and friction work. Gao et al. optimized the shifting process of DCTs, based on minimum impact on the ride comfort and friction work as the target functions to solve the formulated nonlinear constrained problem with offline optimization algorithms [10-11]. Simulation results demonstrated significant reductions of the shifting jerk and sliding friction energy loss. Ye et al. [12] developed a coordinated optimal controller by considering the existing difficulties in motor control and the overlap of a friction clutch, and bench tests verified the control performance. Liang et al. [13] designed a real-time shifting control strategy for a dual input clutch-less transmission. Roozegar et al. [14] proposed a two-phase approach to conduct an optimal control of the shifting process in electric drivelines. In this way, the gains of two independent proportional-integral-derivative (PID) controllers were adjusted by trial-and-error and the genetic algorithm. Simulation results showed that an ideal shifting process quality can be reached despite some external disturbances [3, 15-16].

In this work, an electric drive variable speed (EDVS) system with a novel electromechanical clutch actuator is proposed for better performance in terms of acceleration time and energy economy. The wet clutch is accurately controlled through a shifting mechanism instead of a hydraulic system for smooth shifting. The trajectory tracking control for the driving motor and shifting motor is realized by implementing a double closed-loop control strategy, as shown further below. For smooth clutch engagement, a controller based on a linear quadratic regulator (LQR) method is added with consideration of jerk and friction work. The sliding friction work reaches 11.5 kJ during downshifting, which is reduced by half before optimization. Through simulations and experiments, the effectiveness of the proposed optimization method is validated for acquiring smooth shift quality of the EDVS system.

In Section 2 of this paper, the structure and working principle of the EDVS system with a novel electromechanical clutch actuator are introduced. In Section 3, the dynamic equation of the shifting process is established, and a linear quadratic performance functional is introduced by considering multiple objectives. In Section 4, a weighted matrix is appropriately tuned, and an LQR algorithm solves the problem of optimal control trajectory of the formulated multi-objective functional. In Section 5, details of our test bench are presented, including

the proposed double-loop feedback control method for the drive motor and shifting motor. Section 5 also provides a comparative analysis with the simulation results.

2 THE WET-TYPE TWO-SPEED DUAL-BRAKE TRANSMISSION

2.1 Structure and Operation Principle

The transmission mechanism proposed in this paper is shown in Fig. 1. The transmission uses Simpson-type planetary gear train consisting of a sun gear, two ring gears, and three planet gears for each ring gear. Two different gear ratios can be obtained by braking different ring gears, R1 and C1R2. The input of the mechanism is the sun gear of planetary gear set, S1S2, which is attached to traction motor. The output of the transmission is the carrier of the second stage planetary gear set, C2, which is connected to the wheels via the final drive.

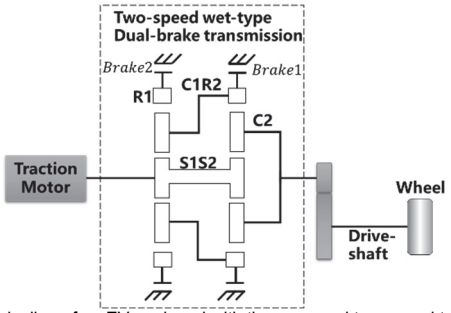

Figure 1 Driveline of an EV equipped with the proposed two-speed transmission

The transmission adopts an electronically controlled motor driving system composed of a shifting motor, a worm gear reducer, and two guide rails. The interface between the worm gear and guide rails is helical. The worm gear is used to convert the rotational motion of the worm into the axial movement of the guide rails, which have helical flanks. In the shifting process, the worm gear is moved along the axial direction for disengaging the current gear and the engagement of the coming gear.

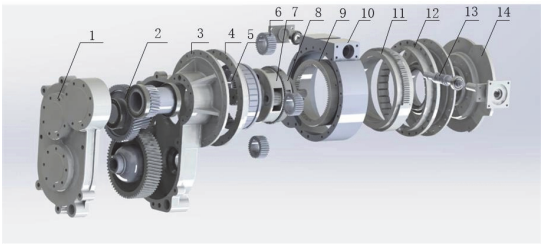

Figure 2 Schematic diagram of the wet-type two-speed dual-brake transmission model (1 - reducer housing, 2 - reducer, 3 - gearbox, 4 - guide rail 1, 5 - sun gear of first stage planetary gear set, 6 - planet gears of first stage planetary gear set, 7 - carrier of second stage planetary gear set, 8 - friction plates, 9 - ring of second stage planetary gear set, 10 - transmission housing, 11 - worm gear, 12 - guide rail 2, 13 - worm, 14 - motor connection flange)

For shifting the gears, each ring gear has brake B1 and B2 operated by an electronically controlled motor driving system to stop each ring gear from spinning. By shifting from Neutral to 1st gear, brake B1 is operated by the shifting motor, and the ring gear of the first stage of the planetary gear set is fixed by the guide rail 1. There is no difference between the shifting mechanism of 1st gear and 2nd gear, except which brake is operated.

The electronic shifting actuator has the advantages of high control accuracy and good adaptability. The shifting motor is a brushless DC motor (BLDC motor) as the power source, which drives the worm gear along the axial direction through the worm shaft. The wet brakes are controlled by a BLDC motor instead of the hydraulic system.

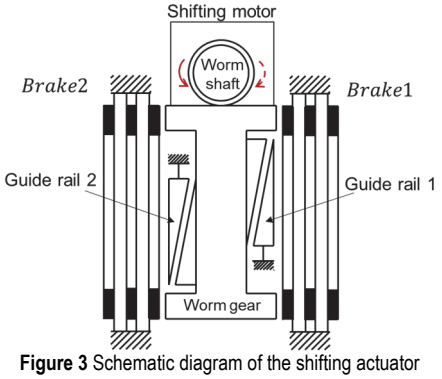

Figure 3 Schematic diagram of the shifting actuator

2.2 Dynamical Model for the Proposed System

The equivalent lever method can be used to establish the dynamic model of the system as long as the lengths of the moment arms and the relationships of contacting gears at different levels for the planetary geartrain are known. The transmission consists of two planetary gear sets, and the whole system is a 2-DOF variable speed mechanism. Therefore, any component's angular velocity can be expressed as a linear combination of the angular velocities of the other two independent components:

$$\omega_j = \alpha_j \omega_A + \beta_j \omega_B \tag{1}$$

where α_j and β_j represent the coefficients of angular velocities determined by the length from j to the endpoints A and B.

We selected S1S2 and C2 as the reference members, and their angular velocities were set equal to 0 and 1, respectively. Based on the arm length between each fulcrum in the lever, the angular velocity of each member relative to the reference member was calculated.

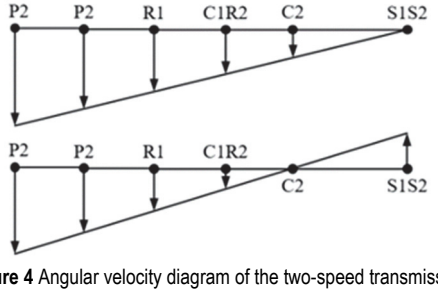

Figure 4 Angular velocity diagram of the two-speed transmission

Using Tab. 1, the angular velocity relationship between each component of the transmission and the reference component can be obtained. Based on the static balance equation of the levers, the dynamic motion equation of the transmission system can be found by using d' Alembert's principle:

$$\left.\begin{aligned}\sum_{j=1}^{n}\alpha_j F_j-\sum_{j=1}^{n}\alpha_j m_j\alpha_j=0\\ \sum_{j=1}^{n}\beta_j F_j-\sum_{j=1}^{n}\alpha_j m_j\beta_j=0\end{aligned}\right\} \tag{2}$$

where F_j represents the force of the component and m_j shows the mass of the component.

Table 1 Coefficients of angular velocities

	α	β
ω_{S1S2}	1	0
ω_{C2}	0	1
ω_{C1R2}	$\frac{Z_{S2}}{-Z_{R2}}$	$\frac{Z_{S2}+Z_{R2}}{Z_{R2}}$
ω_{R1}	$\frac{K\cdot Z_{S1}+Z_{R2}}{-Z_{R2}}$	$\frac{K\cdot Z_{S1}+Z_{R2}+Z_{R2}}{Z_{R2}}$
ω_{p1}	$\frac{K\cdot\frac{Z_{S1}}{Z_{P1}}Z_{R1}+Z_{R2}}{-Z_{R2}}$	$\frac{K\cdot\frac{Z_{S1}}{Z_{P1}}Z_{R1}+Z_{S2}+Z_{R2}}{Z_{R2}}$
ω_{p2}	$\frac{Z_{L2}+Z_{S2}}{-Z_{R2}}$	$\frac{Z_{L2}+Z_{S2}+Z_{R2}}{Z_{R2}}$

Based on the corresponding relationship between the rotating elements and the equivalent linear lever, the dynamic motion equation of the two-speed transmission used in this study can be obtained:

$$\boldsymbol{J}\begin{pmatrix}\dot{\omega}_{S1S2}\\ \dot{\omega}_{C2}\end{pmatrix}=\boldsymbol{A}\begin{pmatrix}T_{S1S2}\\ T_{R1}\\ T_{R2}\\ T_{C2}\end{pmatrix} \tag{3}$$

where matrix $\boldsymbol{J}$ is composed of the angular velocity coefficients and the inertia of each component:

$$\begin{aligned}&J_{11}=\alpha_{S1S2}^2J_{S1S2}+\alpha_{C2}^2J_{C2}+\alpha_{R1}^2J_{R1}+\\&+\alpha_{P1}^2J_{P1}+\alpha_{P2}^2J_{P2}\\&J_{12}=J_{21}=\alpha_{C2}\beta_{C2}J_{C2}+\alpha_{R1}\beta_{R1}J_{R1}+\\&+\alpha_{P1}\beta_{P1}J_{P1}+\alpha_{P2}\beta_{P2}J_{P2}\\&J_{22}=\beta_{C1R2}^2J_{C1R2}+\beta_{C2}^2J_{C2}+\beta_{R1}^2J_{R1}+\\&+\beta_{P1}^2J_{P1}+\beta_{P2}^2J_{P2}\\&A=\begin{pmatrix}\alpha_{S1S2}&\alpha_{R1}&\alpha_{C1R2}&0\\0&\beta_{R1}&\beta_{C1R2}&-\beta_{C2}\end{pmatrix}\end{aligned} \tag{4}$$

When the brake is operated, based on Eq. (3), it means that the relative speed of plates is zero and the static torque of the brakes, T_{R1} and T_{R2}, can be deduced by the following equation:

$$\begin{bmatrix}\dot{\omega}_{S1S2}&\dot{\omega}_v\end{bmatrix}=\left[B\begin{bmatrix}T_{S1S2}&T_{R2}&T_{R1}&T_{C2}\end{bmatrix}^T\right]^T \tag{5}$$

$$\begin{bmatrix}\dot{\omega}_{C1R2}&\dot{\omega}_{R1}\end{bmatrix}=\left[\begin{bmatrix}\alpha_{C1R2}&\beta_{C1R2}\\ \alpha_{R1}&\beta_{R1}\end{bmatrix}\begin{bmatrix}\dot{\omega}_{S1S2}\\ \dot{\omega}_v\end{bmatrix}\right]^T \tag{6}$$

where matrices B and C are determined by the angular velocity coefficients of the two-speed transmission:

$$B=J^{-1}\cdot A \tag{7}$$

$$C=\begin{bmatrix}\alpha_{C1R2}&\beta_{C1R2}\\ \alpha_{R1}&\beta_{R1}\end{bmatrix}\cdot B \tag{8}$$

3 SHIFT CONTROL ALGORITHMS FOR THE WET-TYPE TWO-SPEED DUAL-BRAKE TRANSMISSION

3.1 State-Space Model

By taking the upshifting as an example, the state variables are expressed by $[x_1\,x_2\,x_3\,x_4\,x_5\,x_6\,x_7\,x_8]^T$ consisting of the speed of the driving motor, the relative angle of the transmission, the rotation speed of the driving plates, the output torque of the driving motor, and the transmitting torque of the brake B_2. The control variables are represented by $U=[u_1\,u_2\,u_3]$ including the rate of driving motor output torque changes and the rate of transmission brake torque changes:

$$\begin{cases}x_1=w_{S1S2}\\ x_2=w_v\\ x_3=w_{R2}\\ x_4=w_{R1}\\ x_5=T_{S1S2}\\ x_6=T_{R2}\\ x_7=T_{R2}\end{cases} \tag{9}$$

$$\begin{cases}u_1=\dfrac{\mathrm{d}T_{S1S2}}{\mathrm{d}t}\\ u_2=\dfrac{\mathrm{d}T_{R2}}{\mathrm{d}t}\\ u_3=\dfrac{\mathrm{d}T_{R1}}{\mathrm{d}t}\end{cases} \tag{10}$$

We rearranged the state equations in the form of $\dot{\boldsymbol{X}}=\boldsymbol{MX}+\boldsymbol{NU}+\boldsymbol{V}$, where the matrix $\boldsymbol{M}$ refers to the coefficients of the state variables, the matrix $\boldsymbol{N}$ represents the coefficients of the control variables, and $\boldsymbol{V}$ is the disturbance matrix.

$$\boldsymbol{M}=\begin{bmatrix}0&0&0&0&B_{11}&B_{12}&B_{13}\\0&0&0&0&B_{21}&B_{22}&B_{23}\\0&0&0&0&C_{11}&C_{12}&C_{13}\\0&0&0&0&C_{21}&C_{22}&C_{23}\\0&0&0&0&0&0&0\\0&0&0&0&0&0&0\\0&0&0&0&0&0&0\end{bmatrix},\boldsymbol{N}=\begin{bmatrix}0&0&0\\0&0&0\\0&0&0\\1&0&0\\0&1&0\\0&0&1\end{bmatrix},\boldsymbol{V}=\begin{bmatrix}B_{14}T_{C2}\\B_{24}T_{C2}\\C_{14}T_{C2}\\C_{23}T_{C2}\\0\\0\\0\end{bmatrix} \tag{11}$$

The upshifting process consists of three phases: disengaging phase, free phase, and operating phase. The state-space model for each phase can be expressed as:

1) In the first phase with the brake B_2 disengaged, the friction torque T_{cf} generated by the friction plates of the brake B_1 is equal to the maximum of the static friction torque:

$$T_{cf} = \frac{2}{3}\mu_c N F_{cp} \frac{\left(R_0^3 - R_1^3\right)}{\left(R_0^2 - R_1^2\right)} \tag{12}$$

While the brake B_2 keeps the disengagement status, which means $\dot{\omega}_{B2} = 0$, $T_{R2} = 0$ and $T_{R1} \neq 0$ the dynamic equation of the system can be written as:

$$C_{11} \cdot T_{S1S2} + C_{31} T_{R1} + C_{14} T_{C2} = 0 \tag{13}$$

$$T_{C2} = -\frac{C_{11} \cdot T_{S1S2} + C_{31} T_{R1}}{C_{14}} \tag{14}$$

2) In the free phase, both brakes are disengaged with $T_{R1} = 0$, $T_{R2} = 0$, namely, this stage causes the torque interruption. Therefore, to minimize the interruption duration, the shifting motor is expected to raise the speed to overcome this stage and drive the worm gear to touch the brake B_2 as soon as possible.

3) In the torque phase of the second gear, the brake B_2 is still engaged, and the brake B_1 is disengaged, leading to $\dot{\omega}_{R1} = 0$, $T_{R1} = 0$ and $T_{R2} \neq 0$. Also:

$$C_{21} \cdot T_{S1S2} + C_{22} T_{R2} + C_4 T_{C2} = 0 \tag{15}$$

$$T_{C2} = -\frac{C_{21} \cdot T_{S1S2} + C_{22} T_{R2}}{C_{24}} \tag{16}$$

3.2 Performance Evaluation Index for Shifting

There are two indices to cover the ride comfort and economic performance: the clutch's shifting quality and the service life. The levels of the jerk and sliding friction work are used to evaluate the shifting process. The definition of the jerk is the rate of acceleration change of the vehicle,which is given by the following equation:

$$j = \frac{\mathrm{d}a}{\mathrm{d}t} = \dot{\omega}_v \frac{2\pi r}{60 i_0} = a_1 \frac{\mathrm{d}T_{S1S2}}{\mathrm{d}t} + a_2 \frac{\mathrm{d}T_{B2}}{\mathrm{d}t} + a_3 \frac{\mathrm{d}T_{B1}}{\mathrm{d}t} \tag{17}$$

where j is proportional to the derivative of the motor's and brake transmitted torques. To represent the jerk during the whole shifting process, g_1 is found using the following equation, where t represents the shifting time:

$$g_1 = \int_0^t j^2 \mathrm{d}t \tag{18}$$

The sliding friction work is often used to evaluate the clutch's service life, which is described by the following equation:

$$W = \int_0^{t_1} \left| T_{B1} w_{B1} \right| \mathrm{d}t + \int_0^{t_2} \left| T_{B2} w_{B2} \right| \mathrm{d}t \tag{19}$$

where t_1 shows the moment when the brake B_1 is totally disengaged, t_2 represents the moment when the brake B_2 is totally operated, and w refers to the rotation speed of the plates.

Since there is a trade-off between the above two indexes, the overall evaluation index is set up as shown below, which includes a weight coefficient $\alpha (0 < \alpha < 1)$, to combine the sliding friction work and the jerk. When the weight coefficient is high, it means that there is more emphasis on the jerk term. By tuning the weight coefficient, the simultaneous consideration of the sliding friction work and the jerk is accomplished:

$$Z = \frac{1}{2}\left(W + \alpha \int_0^t j^2 \mathrm{d}t \right) \tag{20}$$

3.3 Linear Quadratic Optimal Control

Due to the interruption of the power transmission, it is necessary to investigate potential solutions to the coordinated shifting process control. The linear quadratic regulator (LQR) method is an optimal control technique which can be described as a unified analytical expression for the standardization of our solution method. The linear state feedback control law is adopted to form a closed-loop optimal control system, which can juggle multiple performance objectives. Based on the dynamic equation of the system and the proposed objective function, optimized trajectories of the driving motor and shifting motor' torques are found through the LQR method. As mentioned before, the jerk and the sliding friction work during gear shifting are considered as the performance evaluation indexes; therefore, our linear quadratic objective function can be expressed as follows:

$$Z = \frac{1}{2}\int_0^t \left| \frac{\mathrm{d}W}{\mathrm{d}t} + \alpha j^2 \right| = \frac{1}{2}\int_0^t \left(X^T Q X + U^T R U \right) \mathrm{d}t \tag{21}$$

When the brake B_2 is disengaged, the weighted matrixes $\boldsymbol{Q}$ and $\boldsymbol{R}$ are calculated and expressed, as follows:

$$\boldsymbol{Q} = \begin{bmatrix} 0 & 0 & 0 & 0 & 0 & 0 & 0 \\ 0 & 0 & 0 & 0 & 0 & 0 & 0 \\ 0 & 0 & 0 & 0 & 0 & 1 & 0 \\ 0 & 0 & 0 & 0 & 0 & 0 & 1 \\ 0 & 0 & 0 & 0 & 0 & 0 & 0 \\ 0 & 0 & 0 & 0 & 0 & 0 & 0 \\ 0 & 0 & 0 & 0 & 0 & 0 & 0 \end{bmatrix}, \boldsymbol{R} = \alpha \begin{bmatrix} \alpha_1^2 & 0 & \alpha_1 \alpha_3 \\ 0 & 0 & 0 \\ \alpha_1 \alpha_3 & 0 & \alpha_3^2 \end{bmatrix} \tag{22}$$

While the brake B_1 is disengaged, the weighted matrixes $\boldsymbol{R}$ is different as shown below:

$$\boldsymbol{R} = \alpha \begin{bmatrix} \alpha_1^2 & \alpha_1 \alpha_2 & 0 \\ \alpha_1 \alpha_2 & \alpha_2^2 & 0 \\ 0 & 0 & 0 \end{bmatrix} \tag{23}$$

Through the LQR method, optimized control variables, trajectories of the driving motor torque, and the transmitted torque of the brake can be calculated using the following equations:

$$U = -KX = -R^{-1}B^T PX \tag{24}$$

$$PA + A^T P - PBR^{-1}B^T P + Q = 0 \tag{25}$$

1) Disengaging phase of brake B_2

Because the transmitted torque of the brake B_2 is zero, the final condition in this case is described as $x_6(t_n) = 0$. The matrix $\boldsymbol{R}$ is associated with the control effort, which restricts the rates of changes of the driving motor's torque and the brake's torque. The selection of the coefficients of R requires considering the variations of the motor torque per unit time and the brake's torque changes. Also, the weight coefficient is found to keep the control input values within the same threshold range. Considering the effects of the weighting matrixes, $\boldsymbol{R}$ is assigned in MATLAB as

$$R = \begin{bmatrix} 2 & 0 & 4\sqrt{3} \\ 0 & 0 & 0 \\ 4\sqrt{3} & 0 & 12 \end{bmatrix}.$$

2)Free phase

Having the electromechanical actuator's characteristics, the rotation speed of the BLDC motor is known both at the beginning and final states. To improve the ride comfort and achieve the desired final states of the rotation speed, we refer to the study by Roozegar [17] about optimizing shifting control. By comparing different fitting curves with various orders, an optimal fitting curve is selected according to the jerk and shifting time requirements. In this study, the 5thorder fitting curve is used to fit the objective trajectory for the rotation speed of the shifting motor in the free phase.

During the shifting, the initial state and final state are given by the following equations:

$$x(t_0) = 0 \tag{26}$$

$$\dot{x}(t_0) = 0\, \dot{x}(t_f) = 0 \tag{27}$$

To determine the angular displacement trajectory $x(t)$, the 5thorder fitting curve $s(\tau)$ are utilized. Thus, $x(t) = \Delta x s(t) + x_0$, where $\tau = t - t_0 / t_f - t_0$, $\tau_0 = 0$ and $\tau_f = 1$. We assume that $s(t) = ft^5 + gt^4 + ht^3 + lt^2 + mt + n$, where f, g, h, d, l, m and n represent the unknown coefficients, respectively. According to the requirements of the trajectory $x(t)$, the fitting curve is given by:

$$s(t) = 6t^5 - 15t^4 + 10t^3 \tag{28}$$

where $0 \le s(\tau) \le 1, 0 \le \tau \le 1$, $\tau = t - t_0 / T$ and $T = t_f - t_0$. The obtained rotation speed of the shifting motor is demonstrated in Fig. 5.

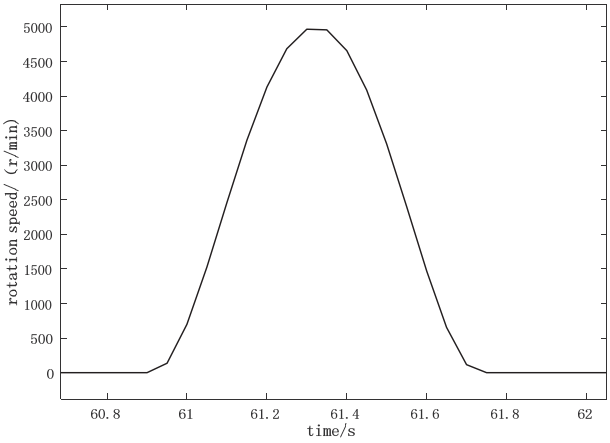

Figure 5 Rotation speed of the BLDC motor during shifting

2) Operating phase of brake B_1

As mentioned before, the rotation speed of the brake B_1 is zero in this case, and as a result, the final condition is described as $x_7(t_n) = 0$. Considering the impact of the weighted matrixes, R is assigned in MATLAB as

$$R = \begin{bmatrix} 195 & 334 & 0 \\ 334 & 1150 & 0 \\ 0 & 0 & 0 \end{bmatrix}.$$

4 SIMULATION RESULTS AND ANALYSIS

The proposed coordination of the optimal control trajectories is described in this section using the dynamic model of the EDVS system established in the previous section. It is necessary to evaluate the control variables deduced by the LQR method in terms of the riding comfort during the shifting based on our simulation model. To verify the advantages of the optimized torques of driving motor and clutches, the trajectories generated by the LQR approach involving the two control variables are described in detail. Besides, a comparison between the control without the optimization technique and the optimized one is conducted. We also compare the optimization results for the two control variables with the previous result that we took only the driving motor's torque into account.

4.1 Downshift Control

In the previous section, the rate of the driving motor's torque changes was considered in the LQR method as the input of the model while another control variable, the clutch's torque, was not included as the input variable directly. To overcome this weakness, the torque is replaced with the rotation speed of the BLDC motor and we run simulations where the original trajectories are regarded as our benchmarks, implemented with a linear fitting for the motor's torque and the 3rdorder fitting for the rotation angle of BLDC's shifting motor shown by the dotted line in Fig. 6. Fig. 6a and Fig. 6b describe the control variables in the downshifting.

During the downshifting, the optimal control variables are applied to avoid non-smooth operations. As it can be seen from Fig. 6c and Fig. 6d, the maximum values of the jerk and the sliding friction work reach 11 m/s^3 and 11,5 KJ, respectively. It is evident that the simulation result with

the original single control variable is inferior, for which the maximum value of the jerk achieves 21,5 m/s^3. Also, the friction work of the cultch for the original control case is twice as much as that for the two variable control cases.

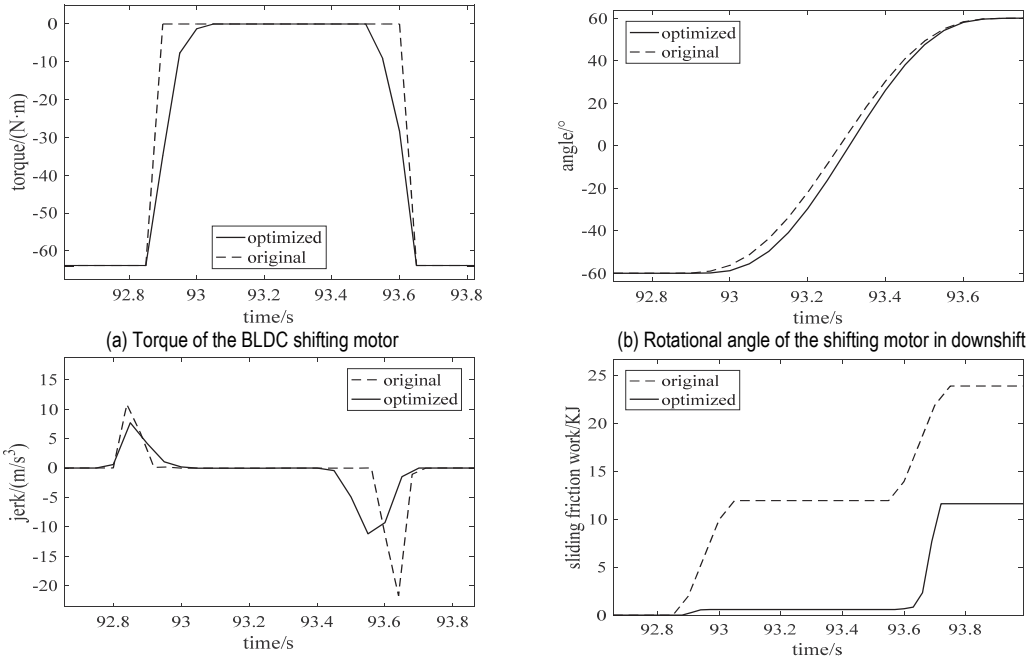

(a) Torque of the BLDC shifting motor

(b) Rotational angle of the shifting motor in downshift

(c) Jerk in downshift

(d) Sliding friction work in downshift

Figure 6 Simulation results in the downshift

4.2 Upshift Control

The comparison of the results in the upshifting case is revealed in Fig. 7. The results indicate that the optimized control input trajectories lead to low levels of the jerk and the clutch friction work. Consequently, the LQR method appears to smooth the shifting by considering the service life of clutch plates. In the upshifting process, when the driving motor participates in the coordinated control scheme, the level of the maximum jerk decreases by 33.3%, and the sliding friction work decreases by 22%. This demonstrates that the coordinated shift motor control in combination with the drive motor during the shifting process reduces the undesirable impacts and the sliding friction work to achieve the smooth shifting.

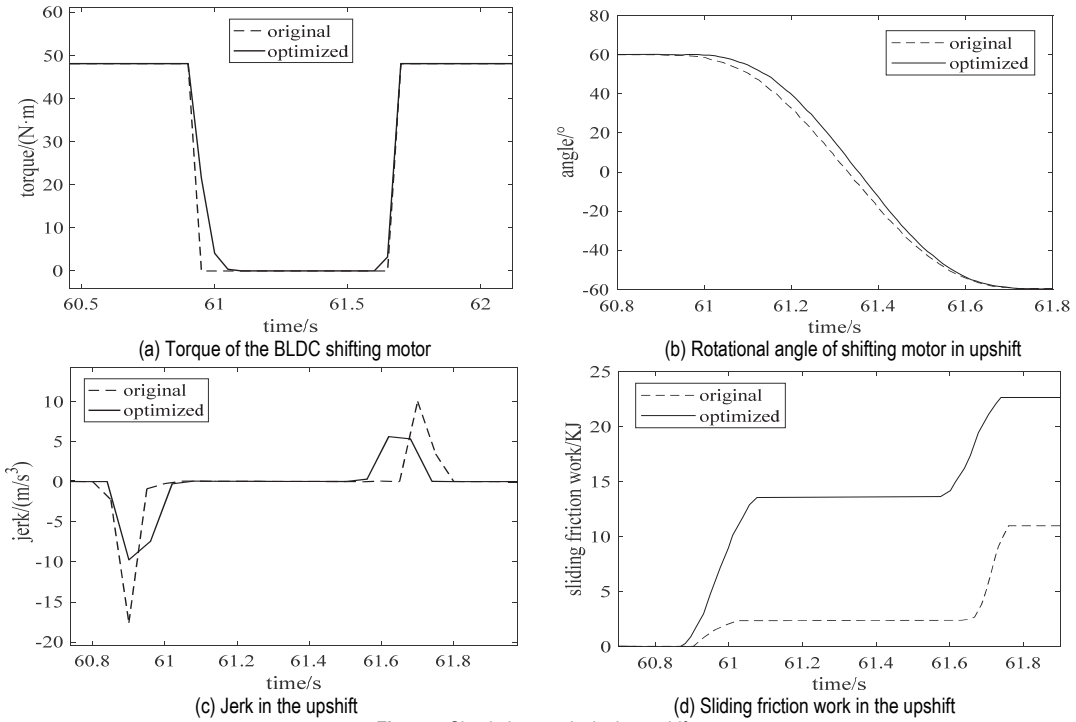

(a) Torque of the BLDC shifting motor

(b) Rotational angle of shifting motor in upshift

(c) Jerk in the upshift

(d) Sliding friction work in the upshift

Figure 7 Simulation results in the upshift

5 EXPERIMENTS

5.1 Test Bench

The prototyping of the proposed EDVS system with a two-speed transmission system including an electromechanical shifting actuator, two brakes, and a Simpson gear set was done in our laboratory. As depicted in Fig. 8, the test bench is composed of a driving motor, a shifting BLDC motor, batteries, two-speed transmission, torque and speed sensors, and an electric dynamometer. In addition, the test setup includes controllers of the motors, control panel, a personal computer, and USB-CAN, in which a NI-CRIO serves as the transmission control unit. The optimized trajectories are embedded into this controller, and the signals of torque and speed are collected for the transmission output shaft through the CAN bus.

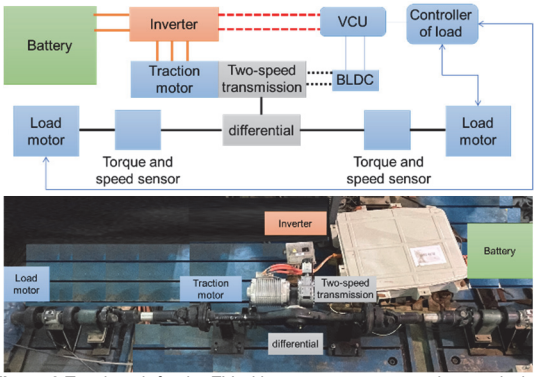

Figure 8 Test bench for the EV with a wet-type two-speed transmission

5.2 Experimental Results

The test bench was used to evaluate the performance of the EDVS system for smooth shifting. First, the optimal control strategy with only the shifting motor as the input is investigated using our test bench. Based on the flow diagram of the TCU module, the optimal control strategy is implemented for the shifting process by focusing only on the shifting motor when the speed of the driving motor is approximately 2455 rpm.

In addition, several experiments were performed using the optimized trajectories of both the driving and shifting motors found by the LQR algorithm that involve the two control-input variables. We implemented a PID controller for tracking the optimized trajectory for the shifting motor. Furthermore, double-closed-loop PI control of the speed torque was carried out for the BLDC, while the outer loop was for the speed and the inner loop for the current. The output speed of the rotor was taken as the input variable for the speed loop.

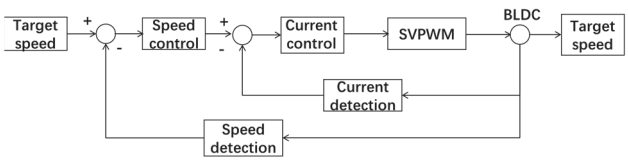

Figure 9 Double closed-loop control diagram of the shifting motor (BLDC)

The test results of downshifting are shown in the following Fig. 10. The downshift starts at 62,9 and ends at 63,8 s; thus, the duration was approximately 0,9 s. During shifting, the maximum value of the jerk was 12,5 m/s^3. Based on the test results, the maximum value of the jerk decreases by 31%, consistent with the simulation results (dotted line) shown in Fig. 7a.

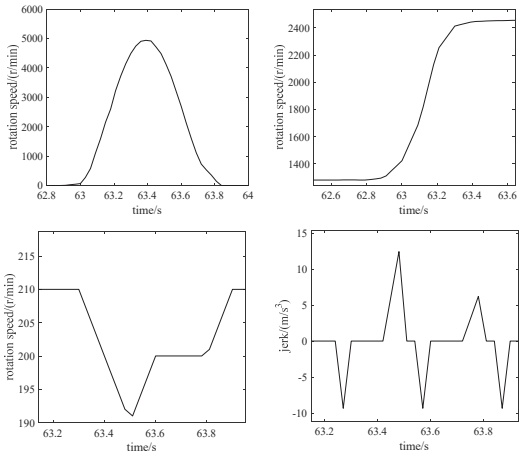

Figure 10 Test results

6 CONCLUSIONS

In this work, using a dynamic model, the optimal shift control problem was transformed into an LQR formulation for the control of the driving and shift motors. The LQR algorithm was applied to optimize the shifting process for minimizing an overall objective function, including the jerk of the vehicle and the friction work of the clutches. We selected/tuned the coefficients of matrix $\boldsymbol{R}$ by considering the control efforts, and the resulting multi-objective optimal control problem was solved accordingly. The superiority of the coordinated control for the gear-shifting process was demonstrated in simulations by analyzing the level of the impact on the smooth operations and sliding friction work. The two-variable linear quadratic coordinated control of the gear-shifting and driving motors was compared with the single-variable linear quadratic optimal control of the gear-shifting actuator during the gear-shifting process. Results based on considering the shifting and driving motors indicated low peak values of the jerk and friction work of the clutches during shifting. Overall, the proposed coordination control was capable of acquiring smooth shifts in terms of ride comfort and service life of the clutches.

Additionally, a test bench was built in our laboratory to assess the devised optimal control strategies. First, an experiment was conducted based on the optimized shifting motor's torque. Results illustrated that the duration of shifting was approximately 0,9 s, and the maximum value of the jerk was in agreement with simulation results. Moreover, another test was conducted to evaluate the LQR algorithm with two control input variables. The maximum value of the jerk decreased by 34%, which was also consistent with simulation results. As a result, the LQR algorithm with two control variables could obtain smooth and swift shifts in both simulations and experiments for the considered EV powertrain system.

Acknowledgements

This work was financially supported by the National Natural Science Foundation of China (Grant No.

51905031), the Fundamental Research Funds for the Central Universities of China, under the Grant No. FRF-FRF-IDRY-20-037A2, Teachers International Exchange Development Program of USTB, QNXM20210027 and the National Key Research and Development Program No. 2018YFC0604402.

7 REFERENCES

[1] Hong, S., Son, H., Lee, S., Park, J., Kim, K., & Kim, H. (2016). Shift control of a dry-type two-speed dual-clutch transmission for an electric vehicle. *Proceedings of the Institution of Mechanical Engineers Part D Journal of Automobile Engineering,* 0954407015585686. https://doi.org/10.1177/0954407015585686

[2] Zhao, Z., Fu, S., Jiang, S., & Lei, D. (2020). Optimal control of mode transition from hybrid to electric mode under turning deceleration conditions for four-wheel-drive HEV with DCT. *Vehicle System Dynamics,* 1-20. https://doi.org/10.1080/00423114.2020.1817506

[3] Roozegar, M. & Angeles, J. (2018). A two-phase control algorithm for gear-shifting in a novel multi-speed transmission for electric vehicles. *Mechanical Systems and Signal Processing, 104*(MAY1), 145-154. https://doi.org/10.1016/j.ymssp.2017.10.032

[4] Tian, Y., Ruan, J., Zhang, N., Wu, J., & Walker, P. (2018). Modelling and control of a novel two-speed transmission for electric vehicles. *Mechanism & Machine Theory, 127*, 13-32. https://doi.org/10.1016/j.mechmachtheory.2018.04.023

[5] Guo, L., Gao, B., & Hong, C. (2016). Online shift schedule optimization of 2-speed electric vehicle using moving horizon strategy. *IEEE/ASME Transactions on Mechatronics, 21*(6), 1-1. https://doi.org/10.1109/TMECH.2016.2586503

[6] Loveday, E. (2009). Retrieve from https: // www. greencarcongress.com /2009 /05 /vocis20090512.html

[7] Spanoudakis, P. & Tsourveloudis, N. C. (2015). Prototype variable transmission system for electric vehicles: energy consumption issues. *International Journal of Automotive Technology, 16*(3), 525-537. https://doi.org/10.1007/s12239-015-0054-x

[8] Liu, F., Chen, L., Yao, J., Lee, C., Kao, C. K., & Samie, F., et al. (2017). Design, modeling, and analysis of wedge-based actuator with application to clutch-to-clutch shift. *Proceedings of the Institution of Mechanical Engineers Part D Journal of Automobile Engineering,* 095440701772717. https://doi.org/10.1177/0954407017727178

[9] Oh, J. J., Kim, J., & Choi, S. B. (2016). Design of self-energizing clutch actuator for dual-clutch transmission. *IEEE/ASME Transactions on Mechatronics, 21*(2), 795-805. https://doi.org/10.1109/TMECH.2015.2474855

[10] Gao, B., Liang, Q., Xiang, Y., Guo, L., & Chen, H. (2015). Gear ratio optimization and shift control of 2-speed i-amt in electric vehicle. *Mechanical Systems and Signal Processing, 50-51*, 615-631. https://doi.org/10.1016/j.ymssp.2014.05.045

[11] Gao, B., Xiang, Y., Chen, H., Liang, Q., & Guo, L. (2015). Optimal trajectory planning of motor torque and clutch slip speed for gear shift of a two-speed electric vehicle. *Journal of Dynamic Systems Measurement & Control, 137*(6), 1-9. https://doi.org/10.1115/1.4029469

[12] Ye, J., Huang, X., Zhao, K., & Liu, Y. (2017). Optimal coordinating control for the overlapping shift of a seamless 2-speed transmission equipped in an electric vehicle. *Proceedings of the Institution of Mechanical Engineers Part I Journal of Systems and Control Engineering, 231*(10), 797-811. https://doi.org/10.1177/0959651817730176

[13] Liang, J., Yang, H., Wu, J, Nong, Z., & Walker, P. D. (2018). Shifting and power sharing control of a novel dual input clutchless transmission for electric vehicles. *Mechanical Systems and Signal Processing, 104*, 725-743. https://doi.org/10.1016/j.ymssp.2017.11.033

[14] Roozegar, M., & Angeles, J. (2017). The optimal gear-shifting for a multi-speed transmission system for electric vehicles. *Mechanism and Machine Theory, 116*, 1-13. https://doi.org/10.1016/j.mechmachtheory.2017.05.015

[15] Fang, S., Jian, S., Song, H., Tai, Y., Fei, L., & Nguyen, T. S. (2016). Design and control of a novel two-speed uninterrupted mechanical transmission for electric vehicles. *Mechanical Systems and Signal Processing, 75*(Jun.), 473-493. https://doi.org/10.1016/j.ymssp.2015.07.006

[16] Zhou, B., Zhang, J., Gao, J., Yu, H., & Liu, D. (2018). Clutch pressure estimation for a power-split hybrid transmission using nonlinear robust observer. *Mechanical Systems and Signal Processing, 106*, 249-264. https://doi.org/10.1016/j.ymssp.2018.01.001

[17] Roozegar, M., Setiawan, Y. D., & Angeles, J. (2017). Design, modelling and estimation of a novel modular multi-speed transmission system for electric vehicles.*Mechatronics, 45*, 119-129. https://doi.org/10.1016/j.mechatronics.2017.06.002

8 APPENDIX

Z refers to the number of teeth of gears and the subscripts *ZS*, *ZP* and Z_R represent the sun gear, pinion, and ring gear.

Contact information:

Xinxin ZHAO, Associate Professor
(Corresponding author)
School of Mechanical Engineering,
University of Science and Technology Beijing,
Beijing, 100083, China
E-mail: xinxinzhao@ustb.edu.cn

Jinggang ZHANG
School of Mechanical Engineering,
University of Science and Technology Beijing,
Beijing, 100083, China
E-mail: g20208614@xs.ustb.edu.cn

Nasser Lashgarian AZAD, Associate Professor
Departmentof system design,
University of Waterloo, Canada
E-mail: nlashgarianazad@uwaterloo.ca

Senqi TAN
School of Mechanical Engineering,
University of Science and Technology Beijing,
Beijing, 100083, China
E-mail: tansenqi@163.com

Yuhan SONG
Linde Hydraulic (China) Co., Ltd,
200 Yongchun Road, Xincheng Street, High-tech Zone, Weifang City,
Shandong, Province, 261205, China
E-mail: songyuhan@weichai.com